NEUROANATOMIE CHIRURGICALE / SURGICAL NEUROANATOMY

A FOCUS ON THE MORPHOMETRY OF THE LABYRINTHINE SEGMENT OF THE FACIAL NERVE CANAL AND THE GENICULATE GANGLION FOSSA ON HIGH-RESOLUTION COMPUTED TOMOGRAPHY : LENGTH AND DIAMETER.

UNE MISE AU POINT SUR LA MORPHOMETRIE DU SEGMENT LABYRINTHIQUE DU CANAL DU NERF FACIAL ET DE LA LOGE DU GANGLION GENICULE AU SCANNER HAUTE-RESOLUTION : LONGUEUR ET DIAMETRE.

FONDJO Teu'mbou Sa'deu [1]
ZUNON-KIPRÉ Yvan Jacques-Olivier Toualy [2]
KAKOU KONAN Médard [2]
VEILLON Francis [3]
NCHUFOR Roland [4]
JIBIA Alain [5]
DJIENTCHEU Vincent de Paul [6]

1. Neurosurgery Unit, Regional Hospital Maroua, Maroua, Cameroon
2. Department of Fundamental Sciences and Bioclinics, Félix HOUPHOUËT-BOIBNY University, Abidjan, Ivory Coast. Neurosurgery Unit, University Hospital Yopougon, Abidjan, Ivory Coast.
3. Imaging Unit 1, University Hospitals of Hautepierre, Strasbourg, France
4. Neurosurgery Unit, Regional Hospital Bamenda, Bamenda, Cameroon – Faculty of Health Sciences, University of Bamenda, Bamenda, Cameroon
5. Faculty of Medicine and Biomedical Sciences, University of Garoua, Garoua, Cameroon. Neurosurgery Unit, Central Hospital Yaounde, Yaounde, Cameroon
6. Neurosciences Unit, General Hospital Yaounde, Yaounde, Cameroon. Faculty of Medicine and Biomedical Sciences, University of Yaounde 1, Yaounde, Cameroon

E-Mail Contact - FONDJO Teu'mbou Sa'deu : sadeufondjo@yahoo.com

Keywords : *Facial nerve; Geniculate ganglion; Tomography, X-Ray computed*
Mots clés *: Nerf facial ; Ganglion géniculé ; Tomographie à rayons X.*

ABSTRACT

Objective

The aim was to measure the dimensions of the labyrinthine segment of the facial canal and the geniculate ganglion fossa, through high-resolution computed tomography, which allows thinner slices of the petrous bones, and by using a wider working sample.

Materials and Methods

We used computed tomography slices of 194 healthy adult petrous bones randomly selected. The CT-Scan machine was of 128 slices. We measured the length (mm) and the diameter (mm), and we determined their means, standard deviations and ranges. The paired Student t-test was used to compare the means according to the gender and the side.

Results

The mean length of the LSFC was 2.70 mm ± 0.54 (range 1.54 – 4.48 mm), with no significant difference between male and female (p = 0.52 and p = 0.33) or right-left (p = 0.23). His mean diameter was 0.97 mm ± 0.35 (range 0.44 – 2.19 mm), with no significant difference between male and female (p = 1.1 and p = 0.37) or right-left (p = 0.65).

For the GGF, the mean length was 2.87 mm ± 0.59 (range 1.47 – 5.10 mm), with no significant male-female difference (p = 0.94 and p = 0.68) or right-left (p = 0.49). The mean diameter was 2.07 mm ± 0.42 (range 0.96 – 3.96 mm). We had a male-female significant difference for the diameter on the left (p = 0.01).

Conclusion

We provide a contribution to the knowledge of the morphometry of the LSFC and the GGF.

RESUME

Objectif

L'objectif était de mesurer les dimensions du segment labyrinthique du canal facial et de la fosse du ganglion géniculé, grâce à la tomographie par ordinateur à haute résolution, qui permet des tranches plus fines des os pétreux, et en utilisant un échantillon de travail plus large.

Matériel et méthodes

Nous avons utilisé des coupes de tomographie assistée par ordinateur de 194 os pétreux d'adultes sains choisis au hasard. Les scanners comportaient 128 coupes. Nous avons mesuré la longueur (mm) et le diamètre (mm), et nous avons déterminé leurs moyennes, leurs écarts types et leurs fourchettes. Le test t de Student apparié a été utilisé pour comparer les moyennes en fonction du sexe et du côté.

Résultats

La longueur moyenne du LSFC était de 2,70 mm ± 0,54 (intervalle 1,54 – 4,48 mm), sans différence significative homme-femme (p = 0,52 et p = 0,33) ou droite-gauche (p = 0,23). Son diamètre moyen était de 0,97 mm ± 0,35 (intervalle 0,44 – 2,19 mm), sans différence significative homme-femme (p = 1,1 et p = 0,37) ou droite-gauche (p = 0,65). Pour le GGF, la longueur moyenne était de 2,87 mm ± 0,59 (fourchette 1,47 – 5,10 mm), sans différence significative homme-femme (p = 0,94 et p = 0,68) ou droite-gauche (p = 0,49). Le diamètre moyen était de 2,07 mm ± 0,42 (intervalle 0,96 – 3,96 mm). Nous avions une différence significative homme-femme pour le diamètre à gauche (p = 0,01).

Conclusion

Nous apportons une contribution à la connaissance de la morphométrie du LSFC et du GGF.

INTRODUCTION

The labyrinthine segment of the facial nerve and the geniculate ganglion which is continuous with it, are two nervous structures which are embedded in and protected by one conduit and one osseous cavity of the petrous temporal bone. These respectively are the labyrinthine segment of the facial nerve canal and the geniculate ganglion fossa (lodge) (5,10,14-18).

These two nervous structures can be affected by various pathologies, tumoral pathologies, such as schwannomas (neurilemmomas) of the labyrinthine facial nerve and the geniculate ganglion, meningiomas (16); but also, traumatic pathologies such as facial palsies resulting from petrous bone fractures with fracture lines crossing the geniculate ganglion (1,10,13,14,19).

The radiological diagnosis of these lesions is based on the appreciation of the morphometry of these osseous canals of the petrous bone; precisely through the measurement of their dimensions (lengths and their diameters). In fact, a pathological process in the labyrinthine part of the facial nerve and in the geniculate ganglion results in an enlargement of their osseous containers (16).

The key sign in case of these labyrinthine facial nerve and geniculate ganglion lesions is therefore the presence of a dilation that causes the labyrinthine facial canal or the geniculate ganglion fossa to bulge and make the radiologic diagnosis easier (16).

High-Resolution Computed Tomography (HR CT) is very important to highlight this widening of the labyrinthine facial canal and geniculate ganglion fossa. This requires that the practitioner knows in advance the anatomical variants of the normal, the normal dimensions of these bony canals and their normal lengths and diameters, which are landmarks for the diagnosis and surgical management of these pathologies (16).

The labyrinthine facial canal and geniculate ganglion fossa are landmarks used in surgery to approach and resect small vestibular schwannomas, located within the internal auditory canal, and with preservation of hearing (6-8). Radio-morphometry of these structures is therefore very important to know in order to guide the surgeon in his gestures.

Thus, regarding these normal dimensions of the labyrinthine facial canal and the geniculate ganglion fossa, several types of studies have been conducted on this subject including anatomical studies, as well as histological and radiological studies (on standard radiography, conventional tomography, as well as computed tomography) (3,5,11,12,14-16,18-20).

Concerning the radiological series, most studies on the morphometry of the labyrinthine facial canal and geniculate ganglion fossa, on computed tomography, have been carried out either on small samples (11,13,14,19,20), with scanners which do not allow thin slices of the temporal bone (19,20), using measuring techniques that deviate from the landmarks used for the measurements in anatomical series (12), or on sample materials which do not correspond directly to the petrous bone (19,20).

For example, Wadin and Wilbrand studied the morphometry of the labyrinthine facial canal not with the computed tomography, but with conventional tomography; and not on petrous bone specimens, but on the plastic casts of these (20). Valavanis et al. did the measurements on high-resolution computed tomography, but on a small sample of 05 normal petrous bones (14). Jin et al. studied the anatomical variations of the labyrinthine facial canal also with high-resolution computed tomography, but on a sample of 10 temporal bones (11).

The aim of this study was to provide an update on the morphometry of the labyrinthine facial nerve canal and the geniculate ganglion fossa. To do so, the authors had as objective the measurement of these canals on high-resolution computed tomography, by using a wider working sample, a CT-scan of better precision allowing thinner slices of the petrous bones, and a measuring technique similar to that of anatomical studies. The results obtained were compared with those of previous studies available in the literature, both radiological series, anatomical and histological series.

MATERIALS AND METHODS

Study design

We carried out a retrospective and descriptive study, in the Imaging Unit of the Teaching Hospitals of Hautepierre at Strasbourg in France. The period of recruitment covered one year, from 1rst January to 31rst December 2016.

Materials

Materials of study

The authors used the computed tomography slices of 194 healthy petrous bones (97 adult persons), recruited in the database of the Imaging Unit of the University Hospitals of Hautepierre. They represented 45 males and 52 females (male/female sex ratio: 0.86), with a mean age of 49.3 years, (range 18-83 years).

Criteria of selection

We included in the study, the CT-scan images of all healthy petrous bones of adult subjects, for whom head CT scans were done within the period of study, in the Imaging Service of the University Hospitals of Hautepierre. These were « all-comers » patients, randomly selected.

The petrous bones of any patient presenting neurological signs such as Bell's palsy were not included in the sample, as well as all the petrous bones presenting a lesion (traumatic, infectious or neoplastic). We also excluded from our sample, the petrous bones of all non-adult patients.

Imaging devices

The CT-scan used were *Siemens*®, « *SOMATOM Definition AS + Fast Care* » model, with 128 slices. The working computers were *Apple*®, « *MacIntosh* » model. The images were selected and processed with the medical imaging software « *OsiriX* ».

Methods

Imaging protocol

The protocol used for image acquisition is summarized in Table I, and the one used for the post-treatment in Table II. Native images were manipulated to obtain particular planes in which different variables were studied, and the data were analysed using the statistical analysis software « SPSS 18.0 ».

The studied variables

For each of the two osseous structures, we studied the length (mm) and the diameter (mm).

- **Measurement plans :** The measurements were realized on the axial slices of the petrous bone, in the plane parallel to the semi-circular canal. An axial slice of petrous bones of good quality should highlight on the same image : the ring of the lateral semi-circular canal, the head of the malleus, the body of the incus, the cochlea and the tympanic segment of the facial canal (Figure 1).
- **Measurement techniques :** The measurements were done according the anatomical landmarks used by Lang (12) in his dissections (Figure 2). The length of the labyrinthine facial canal was measured in the medio-lateral direction (Figure 3), by connecting a straight line from the medial to the lateral ends of the canal (distance a-b in Figure 2). Its diameter was measured in the antero-posterior direction (Figure 4), by connecting the anterior and the posterior edges of the canal (distance c-d in Figure 2). We measured the diameter of the mid part of the canal. The length of the geniculate ganglion fossa (distance e-f in Figure 2) was measured in the antero-posterior direction (Figure 5), by connecting the anterior end of the fossa (origin of the greater superficial petrosal nerve) to its posterior end (origin of the tympanic segment of the facial nerve canal). Its diameter was measured in the medio-lateral direction (Figure 6), by connecting its medial edge to the lateral one (distance g-h in Figure 2).

Analysis of the data

We determined for our different variables, the following parameters: mean (mm), standard deviations (mm), and ranges (minimum, maximum). The paired Student *t*-test was used to compare the means of the different parameters, according to the gender (male-female) on one hand, and the side (right-left) on the other. The difference between two means is considered as significant when the *p-value* obtained is less than the threshold value of 0.05.

RESULTS

Labyrinthine Segment of the Facial Canal

Length of the Labyrinthine Segment of the Facial Canal

The mean length of the labyrinthine segment of the facial canal was **2.70** ± 0.54 mm, (range 1.54 – 4.48 mm). There was no significant difference between the mean lengths of males' facial canals (2.65 mm) and of females' facial canals (2.74 mm), $p = 0.52$ on the left and $p = 0.33$ on the right. Likewise, there was no significant difference between the mean lengths of the right facial canals (2.73 mm) and of the left facial canals (2.67 mm), $p = 0.23$.

Diameter of the Labyrinthine Segment of the Facial Canal

The mean diameter of the labyrinthine segment of the facial nerve canal was **0.97** ± 0.35 mm, range 0.44 – 2.19 mm. There was no significant difference between the mean diameter of males' facial canals (1.02 mm) and of females' facial canals (0.93 mm), p = 1.10 on the left and p = 0.37 on the right. Similarly, there was no significant difference between the mean diameters of the right facial canals (0.98 mm) and of the left facial canals (0.97 mm), p = 0.65.

Geniculate Ganglion Fossa

Length of the Geniculate Ganglion Fossa

The mean length of the geniculate ganglion fossa was **2.87** ± 0.59 mm, range 1.47 – 5.10 mm. There was no significant difference between the mean lengths of the geniculate ganglion fossa in males (2.89 mm) and females (2.86 mm), p = 0.68 on the left and p = 0.94 on the right. Similarly, there was no significant difference between the mean lengths of the right geniculate ganglion fossa (2.89 mm) and of the left geniculate ganglion fossa (2.87 mm), p = 0.49.

Diameter of the Geniculate Ganglion Fossa

Concerning the diameter of the geniculate ganglion fossa, the mean diameter was **2.07** ± 0.42 mm, range 0.96 – 3.96 mm. There was a significant difference between the mean diameters of the geniculate ganglion fossa in males and females seen on the left side (***p* = 0.01**), and none on the right (p = 0.58). There was no significant difference between the mean diameters of the right geniculate ganglion fossa (2.05 mm), and of the left geniculate ganglion fossa (2.11 mm), p = 0.16.

DISCUSSION

Since we recruited from the database of « all-comers » patients, our recruitment is thus random. Except for the diameter of the geniculate ganglion fossa for the left petrous bones, no significant difference was found between the means of the variables neither according to the gender (between male and female petrous bones), nor according to the side (between right and left petrous bones). Ours results can therefore be representative of the two petrous bones of any adult subject, both male and female.

High-Resolution CT is the best exam for exploration of the temporal bone cavities and canals (2,5,9,11,12,15,16,18,21). The recommended plane for this exam, which is the one recommended for the exploration of the petrous bone, is the axial plane parallel to the semi-circular canal (2,5,11,12,15,19,21). It's this plane that we used in our study. In addition to allowing a good exploration of the petrous bone canals, it permits us to avoid the irradiation of the lens of the eyes (11,15). This plane of acquisition must pass above the orbits anteriorly and through the petrous bones posteriorly (15).

The examination parameters used in our study are similar to those recommended by authors in the literature for petrous bones computed tomography (2,3,5,9,11,15,18-21).

Labyrinthine Segment of the Facial Canal

Length of Labyrinthine Segment of the Facial Canal

The mean length of the labyrinthine facial canal obtained in our study, **2.70** ± 0.54 mm (ranges 1.54-4.48 mm), is close of those of several authors in the literature, regardless of the type of study.

Indeed, Ge and Spector in their anatomical series on 10 human temporal bones report a mean length of **2.82 mm** (ranges 2.25–3 mm) (21). Lang in anatomy relates also a mean length of **2.81 mm**, with extreme values at 1.5–5.2 mm (12). Their results are near of those of Veillon who reports a mean length of **2.8 mm** (ranges 2.5–5.2 mm) (16-18).

Some authors report a mean length of the labyrinthine facial canal superior to our result, particularly in some radiological series. In their study on the anatomy of the labyrinthine facial canal performed on the plastic casts of 200 temporal bones, Wadin and Wilbrand report a mean length of **3.3 mm** (ranges 1.6-5.9 mm) for this

osseous canal (20). Jin et al. in their study on the variations of the labyrinthine facial canal on High-Resolution CT, on a sample of 10 temporal bones, report a mean length of **3.56 mm** (ranges 2-4 mm) (11).

These differences with our results can be explained by the fact that Wandin and Wilbrand didn't perform all their measurements on High Resolution CT as was done in our study, but they also used standard radiography and conventional tomography (20). Moreover, their measurements of the labyrinthine facial canal were not done directly on human petrous bones, but indirectly on theirs plastic and silicone casts (20). Jin et al. (11) and Valavanis et al. (14) used High-Resolution CT, however their respective samples of 10 and 05 petrous bones are smaller than ours.

Variants of long canals are reported in the literature. Indeed, Jin et al. describe as long labyrinthine facial canal, that of length 6.8 ± 0.38 mm (ranges 5.2-8.3 mm) (11). A high extreme value of 6 mm is also reported by Valavanis et al. (14), who also performed their measurements on High-Resolution CT. On the other hand, according to Veillon, an elongation of the labyrinthine facial canal beyond 5.2 mm, with a stretched aspect, integrates into a malformative context of the labyrinth (16,17).

Weiglein et al. report extreme values for the length of the labyrinthine facial canal between 2.5-6 mm and a diameter between 0.8-2.5 mm (4). Weiglein et al. performed computed tomography slices 1.5 mm thin (more spaced than in our study), on temporal bones of 3 human cadavers and 15 alive adult subjects (4).

For the values of the length of the labyrinthine facial canal according to the side, Lang in his anatomical study reports for the canals of the right petrous bones a mean length of **2.63 mm**, range 1.5-3.3 mm (**2.73 mm** in our study). And for the canals of left petrous bones, a mean length of **3.03 mm**, range 2.1-5.2 mm (**2.67** mm in our study). However, Lang did not perform a test of comparison of the means lengths, and did not determine the lengths of the facial canal according to the gender.

Diameter of the Labyrinthine Segment of the Facial Canal

About the mean diameter of the labyrinthine facial canal, our result **0.97** ± 0.35 mm (range 0.44 – 2.19 mm), is close of the value obtained by Valavanis et al. on High-Resolution CT : **1.02** ± 0.08 mm (range 1.02 – 1.53 mm) (4).

Some authors report a mean diameter superior to ours. Indeed, in the work realized by Wadin and Wilbrand on the plastic casts of 200 temporal bones (20), the mean diameter, measured at the mid part of the labyrinthine facial canal is **1.8 mm** (range 0.91-2.7 mm). The same measurements realized on computed tomography by Wandin in another study on the plastic casts of 10 temporal bones, give a mean diameter of **1.4 mm** (range 1.0–1.8 mm) (19). Lang in anatomy s a mean diameter of **1.47 mm** (range 0.8–2.4 mm) (12).

Despite a considerable sample of 200 temporal bones used by Wadin and Wilbrand in their study, we believe our study provides more accurate values for the labyrinthine facial canal. This stems from the fact that we used more recent imaging tools and techniques, allowing a finer analysis of the petrous bones with more precision in the slices and measurements. As a result, we think our results are closer to reality.

A mean diameter of the labyrinthine facial canal inferior to ours is reported by Veillon et al. in radiology: 0.7 mm (16).

Ge and Spector in their anatomical dissections on 10 human temporal bones has measured the narrowest and the widest parts of the labyrinthine facial canal (21). They report a mean diameter for the narrowest part of the canal of **0.7 mm** (range 0.6-0.9 mm), and for the widest part, 1.12 mm (range 0.9-1.5 mm). This aspect was not appreciated in our study.

In the determination of the mean diameter of the labyrinthine facial canal according to the gender, Lang (12) reports for male petrous bones a value of **1.57 mm**, range 0.95–2.4 mm (**1.02 mm** in our study) ; and for female petrous bones, a mean diameter of **1.24 mm**, range 0.8–1.99 mm, (**0.93 mm** in our study).

According to the side, Lang (12) reports a mean diameter of **1.59 mm** (range 0.9–2.4 mm) for the canals of the rights petrous bones (**0.98 mm** in our study) ; and for the canals of left petrous bones, a mean diameter of

1.34 mm, range 0.8–2.1 mm (0.97 mm in our study). However, Lang did not perform test of comparison for mean diameter of the labyrinthine facial canal, neither by gender nor by side.

A great variability of the mean diameter of the labyrinthine facial canal across the same canal is reported in literature. Lang in his study relates that the mean diameter of the labyrinthine facial canal tends to increase from the medial to the lateral part. He measured in this direction three zones of variation, from the bottom of the internal acoustic meatus to the origin of the geniculate ganglion fossa. He obtained measurements as follows: medial diameter (1.19 mm), central diameter (1.47 mm) and lateral diameter (2.40 mm) (12).

Wadin in his study in radio-anatomy highlights a similar variability of the diameter across the same labyrinthine facial canal. She measured four zones of variation in the diameter, with mean values of: 1.4 mm, 1.5 mm, 1.8 mm and 2 mm. The diameter tends to increase from inside to outside (20).

Ge and Spector measured the diameter of the labyrinthine facial canal in its widest portion (near the geniculate ganglion) and in its narrowest portion (near the internal acoustic meatus) (21). The diameter of the narrowest portion was 0.7 mm (range 0.6-0.9 mm), and that of the widest portion was 1.12 mm (range 0.9-1.5 mm) (21).

Geniculate ganglion fossa

Length of the Geniculate Ganglion Fossa

The mean length of the geniculate ganglion fossa obtained in our study, **2.87** ± 0.59 mm (range 1.47–5.10 mm), is close of that obtained by Lang in anatomy, **2.82 mm** (range 1.9–4.6 mm) (12).

Some authors report a mean length of the geniculate ganglion fossa inferior to ours. Indeed, Dobozi in his series of histological sections report a mean length of **1.09 mm** (3). Ge et Spector in their anatomical series report a mean length of **1.76 mm** (range 1.2–2.25 mm) (21). Veillon et al. on their part report a mean length **2.1 mm** (range 1.8-5 mm) (16).

We can explain these discrepancies between our results, by the great differences in our sample sizes. Indeed, we used in our study, 194 temporal bones, while these authors used samples smaller than ours, namely: 24 temporal bones for Dobozi (3), and 10 for Ge et Spector (21). In addition to having used a sample smaller than ours, Dobozi also included children aged 11 and above in his study (3), while we realized our measurements only on adults aged 18 years and above.

For the mean length of the geniculate ganglion fossa according to the side, Lang (12) reports for the lodges of the right petrous bones a value of **2.54 mm** (range 1.9-4.2 mm), against **2.89 mm** in our study. And for the lodges of the left petrous bones, he reports a mean length of **3.14 mm** (range 2.2-4.6 mm), against **2.87** mm in our study.

However, contrary to our work, Lang did not perform a test of comparison for the mean lengths of the geniculate ganglion fossa according to the side, and he did not determine this mean length according to the gender. The Student's paired *t* test in our study did not highlight a significant difference between the mean lengths neither by side, nor by gender.

Diameter of the Geniculate Ganglion Fossa

The mean diameter of the geniculate ganglion fossa obtained in our study, **2.07** ± 0.42 mm (range 0.96 – 3.96 mm) is different from that obtained by some authors.

Indeed, it's superior to the mean diameter obtained by Dobozi, **0.76 mm** (3) ; as well as the mean diameter obtained by Ge and Spector, **1.29 mm** (range 0.9–1.95 mm) (21).

Lang however reports a mean diameter of geniculate ganglion fossa superior to that of the present study: **3,13 mm** (range 1.8 – 4.5 mm) (12).

We obtained in our study a significant difference between the mean diameters of the geniculate ganglion fossa, for the left petrous bones of men and women. Indeed, the values we obtained with the Student's paired *t* test are p = **0.01** for the left petrous bones, and p = 0.58 for the right petrous bones.

In a radiological study on computed tomography on a series of 107 patients, Xiaofei Mu et al. measured the mean transversal diameter of the geniculate ganglion fossa (13). They did a test of comparison of the diameters according to the side (right-left), with the Student paired *t*-test, and they didn't find a significant difference, the result obtained being p = 0.217.

Applications

The morphometry of the labyrinthine facial canal and the geniculate ganglion fossa has both diagnostic and surgical relevance.

The dimensions and the morphology of these osseous cavities are key elements for the diagnosis of several pathologies of their nervous contents. Indeed, geniculate ganglion tumours such as schwannomas (neurilemmomas), meningiomas, express themselves on computed tomography by a dilatation of their osseous lodge. The measuring of his diameter and the knowledge of the limits of the normal are thus crucial for the diagnosis. Similarly, petrous bone fractures with facial palsy reveal on computed tomography an enlargement of the geniculate ganglion fossa (13). The mean transversal diameter of that fossa in these fractures is 1.9 ± 0.3 mm according to Xiaofei Mu et al. (13).

According to Veillon et al., within the limits of a diameter less than 4.5 mm, it's possible to include the variants of the normal of geniculate ganglions of various forms (17). We find in our study an extreme value for the diameter of geniculate ganglion fossa of 3.96 mm, that we can consider as the cut off point for the diagnosis of these pathologies of the geniculate ganglion or its fossa.

For the labyrinthine facial canal, a tumoral or malformative process cannot be envisaged only on the basis of its dilated appearance on computed tomography (18). Indeed, the shape of the labyrinthine portion of the facial canal is linked to its length. Wadin describes two types of canals: long types which are narrow, and short types which are wide (20).

Consequently, from these findings we should not attribute a pathological character to a short and wide canal (17), especially if its anterior concavity is preserved (16). The measurement of its diameter is the determining element for the diagnosis. The pathological limit is 2.5 mm for the widest diameter according to Veillon (17), and the normal extreme value reported by Lang is 2.4 mm. We found an extreme value of 2.19 mm in our study, that we considered as normal upper limit of the diameter of the labyrinthine facial canal. This value offers a threshold for the suspicion of a pathological process related to the labyrinthine facial canal.

In the literature, there is controversy about the role of the diameter of the labyrinthine facial canal in the pathogenesis of Bell's palsy. Indeed, in a study about the implication of the diameter of the facial canal in this paralysis, Onur Celik et al. compared on computed tomography the canals of the affected nerves, to those of the healthy contro-lateral nerves, on a cohort of 34 temporal bones (1). They concluded that the affected sides presented a mean diameter of the labyrinthine facial canal significantly smaller than that of the healthy sides (1.09 mm for the affected sides against 1.23 mm for the healthy sides, p = 0.00) (1), making the nerves in these canals more fragile.

Wadin et al. (19) compared on computed tomography also (at 1 mm and 2 mm of thick slices), the mean diameters of the labyrinthine facial canal of healthy and sick patients. They compared the mean diameter a sample of 22 canals of patients presenting a Bell's palsy, to the one of a sample of 28 canals of healthy patients; and contrary to Onur Celik et al., they reported that there was no significant difference in the mean labyrinthine facial canal diameter between the affected and the healthy sides (19).

The dimensions of these osseous cavities are also relevant in surgery. In neurosurgery, the House's technique is a procedure used to approach and remove intra-canalar vestibular schwannomas (neurilemmomas) with no hearing loss (6-8). During this process, through a sub-temporal approach, the roof of the geniculate ganglion fossa and that of the labyrinthine facial canal are drilled successively, from outside inward, in order to guide the surgeon and allow him to reach the internal acoustic meatus where the tumor is localed. With the pre-

operative knowledge of the lengths of the labyrinthine facial canal and the geniculate ganglion fossa, the surgeon knows in advance what length of bone to drill before reaching the tumor.

For the purpose of preserving hearing most especially, pre-operative knowledge of the labyrinthine facial canal diameter is crucial. Indeed, the cochlea is close and anterior to this canal. It is thus important for the surgeon to know in advance how much bone to drill without causing injury the cochlea in front.

CONCLUSION

The authors provide in this study an update about the radio-morphometry (dimensions) of the labyrinthine segment of the facial nerve canal and the geniculate ganglion fossa. This was done on the basis of High-Resolution computed tomography, which allows for greater precision in the radiological anatomy of the petrous bone canals, by giving more thinner slice ; and also, on the basis of a larger study sample compared to those of previous studies available in the literature.

The authors also contribute to enrich the anatomical knowledge of these structures, with the determination and comparison of the means of the variables (length, diameter), by gender and by side. We think that more precise and reliable values of these osseous canals can be obtained with further studies on greater samples.

Table I : Protocol used for computed tomography of petrous bones

Patient Installation	**Supine position, head in hyperflexion.**	
Explored Zone	From the internal acoustic meatus to the outlet of the petrous bones.	
Scout View		
Voltage	120 kV	
Intensity	36 mA	
CT Parameters		
Voltage	140 kV	
Intensity	400 mA	
Number of Detector	16	
Thickness of the nominative cuts	0.3 mm	
Thickness of the reconstructed cuts	0.4 mm	
Interval of reconstruction	0.1 mm	
Pitch	0.45	
Filter of reconstruction	U 75 very hard ASA	
Windows W/L	4000 / 700 UH	
Delay	2	
Reconstructions		
	Right petrous bone	Left petrous bone
Thickness of the cuts	0.4 mm	0.4 mm
Interval of reconstruction	0.1 mm	0.1 mm
Filter of reconstruction	U 75 very hard ASA	U 75 very hard ASA
Window W/L	4000 / 700 UH	4000 / 700 UH
Computed Tomography Dose Index Volume	132 mGy	

The acquisition of the images was done according to these computed tomography parameters.

Table II : Post-treatment of computed tomography images of petrous bones

Axial Reconstruction	**60 images**
	0.4 mm of thickness of the image
	0.3 mm of distance between images
Sagittal Reconstruction	60 images
	0.4 mm of thickness of the image
	0.3 mm of distance between images
Coronal Reconstruction	60 images
	0.4 mm of thickness of the image
	0.3 mm of distance between images
Zoom 10	60 images
	0.4 mm of thickness of the image
	0.2 mm of distance between images
VO	5 images
	0.4 mm of thickness of the image
	0.2 mm of distance between the images

The post-treatment of the images was done according to these computed tomography parameters.

Table III : Length of the labyrinthine segment of the facial nerve canal according to the sex and the side

	Length of the labyrinthine segment of the facial canal (n = 194)			
	Sex		Side	
	Male	Female	Right Petrous bone	Left Petrous bone
	(n = 90)	(n= 104)	(n = 97)	(n = 97)
Mean (mm)	2.65	2.74	2.73	2.67
Minimum (mm)	1.58	1.54	1.65	1.54
Maximum (mm)	3.93	4.48	4.35	4.48
Standard deviation	0.54	0.56	0.52	0.58
***p*-value (Paired Student's *t*-test)**	*p* on the left side: 0.52 *p* on the right side: 0.33		0.23	

There was no significant difference between the mean lengths of males' and females' facial canals, $p = 0.52$ on the left and $p = 0.33$ on the right. Similarly, there was no significant difference between the mean lengths of right and left facial canals, $p = 0.23$.

Table IV : Diameter of the labyrinthine segment of the facial nerve canal according to the sex and the side

	Diameter of the labyrinthine segment of facial canal (n = 194)			
	Sex		Side	
	Male	Female	Right petrous bone	Left petrous bone
	(n = 90)	(n = 104)	(n = 97)	(n = 97)
Mean (mm)	1.02	0.93	0.98	0.97
Minimum (mm)	0.44	0.47	0.47	0.44
Maximum (mm)	2.19	2.17	2.19	2.11
Standard deviation	0.34	0.36	0.36	0.34
***p*-value (Paired Student's *t*-test)**	*p* on the left side: 1.10 *p* on the right side: 0.37		0.65	

There was no significant difference between the mean diameter of males' and females' facial canals, $p = 1.10$ on the left and $p = 0.37$ on the right. Likewise, there was no significant difference between the mean diameters of right and left facial canals, $p = 0.65$.

Table V : Length of the geniculate ganglion fossa according to the sex and the side

	Length of geniculate ganglion fossa (n = 194)			
	Sex		Side	
	Male	Female	Right petrous bone	Left petrous bone
	(n = 90)	(n = 104)	(n = 97)	(n = 97)
Mean (mm)	2.89	2.86	2.89	2.87
Minimum (mm)	1.47	1.50	1.60	1.47
Maximum (mm)	5.10	4.59	4.59	5.10
Standard deviation	0.56	0.64	0.58	0.62
***p*-value (Paired Student's *t*-test)**	*p* on the left side: 0.68 *p* on the right side: 0.94		0.49	

There was no significant difference between the mean lengths of males and females geniculate ganglion fossa, $p = 0.68$ on the left and $p = 0.94$ on the right. There was no significant difference between the mean lengths of right and left geniculate ganglion fossa, $p = 0.49$.

Table VI : Diameter of the geniculate ganglion fossa according to the sex and the side

	Diameter of the geniculate ganglion fossa (n = 194)			
	Sex		Side	
	Male	Female	Right petrous bone	Left petrous bone
	(n = 90)	(n = 104)	(n = 97)	(n = 97)
Mean (mm)	2.15	2.02	2.05	2.11
Minimum (mm)	0.96	1.13	0.96	1.22
Maximum (mm)	3.96	3.02	3.96	3.02
Standard deviation	0.58	0.36	0.46	0.39
***p*-value (Paired Student's *t*-test)**	*p* on the left side: **0.01** *p* on the right side: 0.58		0.16	

There was a significant difference between the mean diameters of males and females geniculate ganglion fossa seen on the left side (***p* = 0.01**), but not on the right (*p* = 0.58). However, there was no significant difference between the mean diameters of right and left geniculate ganglion fossa, *p* = 0.16.

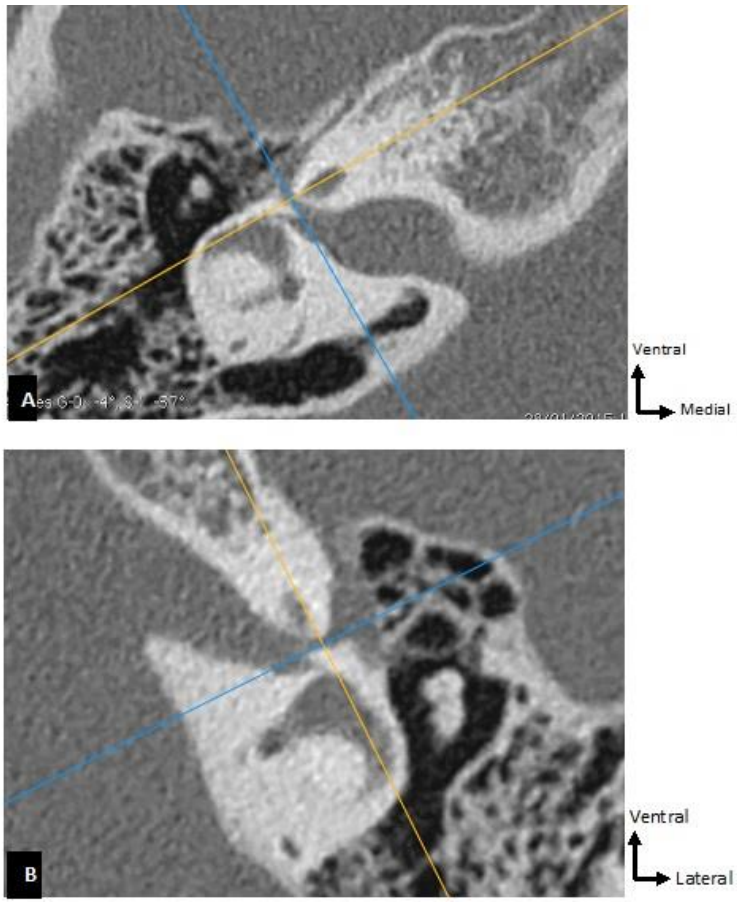

Fig. 1 : Axial slices of petrous bones, parallel to the lateral semi-circular canal, used to measure the dimensions of the labyrinthine segment of facial nerve canal and the genicu-late ganglion fossa. These slices highlight on the same image, the ring of the lateral semi-circular canal, the head of the malleus, the body of the incus, the cochlea and the tympanic segment of the facial canal. A. Right petrous bone; B. Left petrous bone.

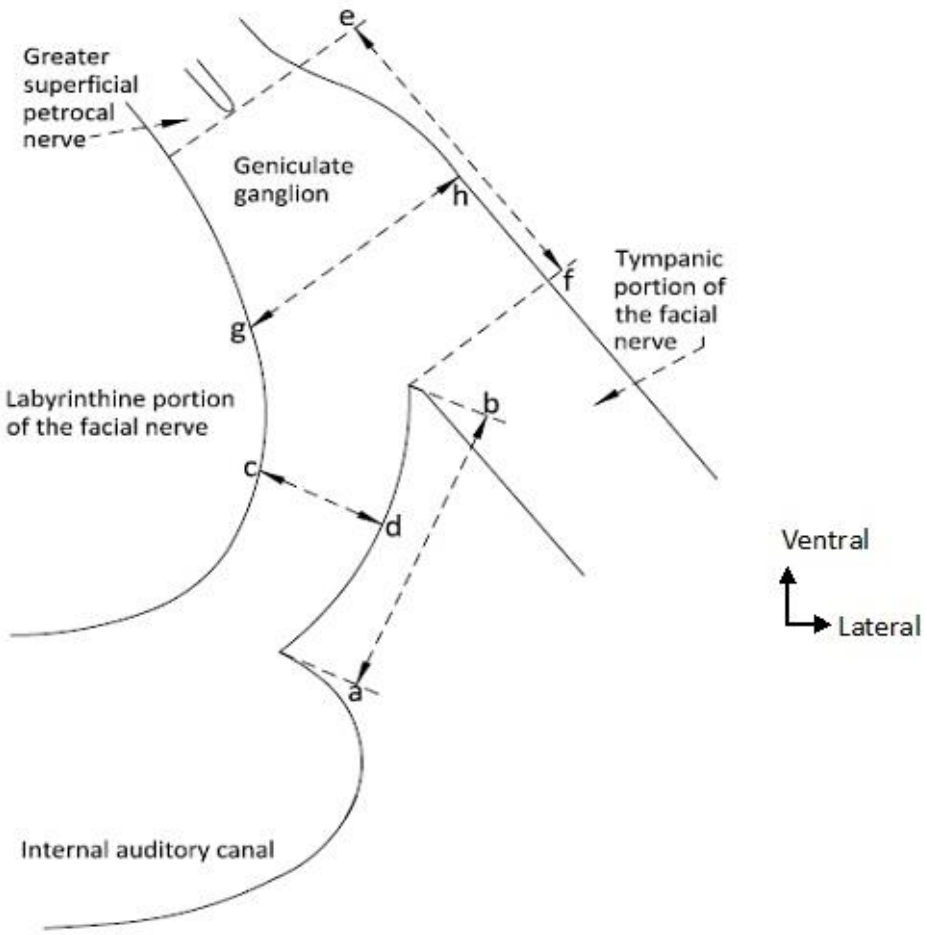

Fig. 2 : Illustration of the landmarks used for the measurements of the labyrinthine seg-ment of the facial canal and the geniculate ganglion fossa.
a – b : Length of the labyrinthine segment of the facial canal ;
c – d : Diameter of the labyrinthine segment of the facial canal ;
e – f : Length of the geniculate ganglion fossa ;
g – h : Diameter of the geniculate ganglion fossa.

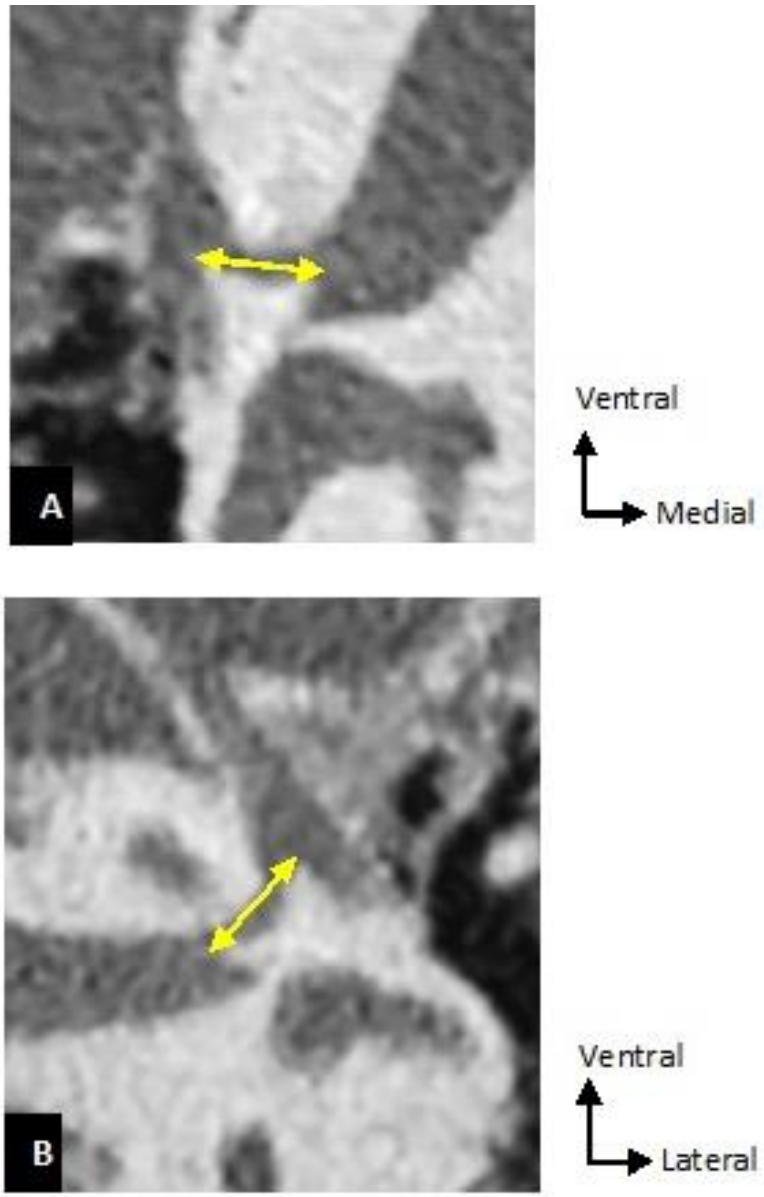

Fig. 3 : Illustration of the measurement of the length of the labyrinthine segment of facial canal on an axial slice of the petrous bone. The measurement is made on a straight line link-ing the two ends of the facial canal. A. Left petrous bone; B. Right petrous bone.

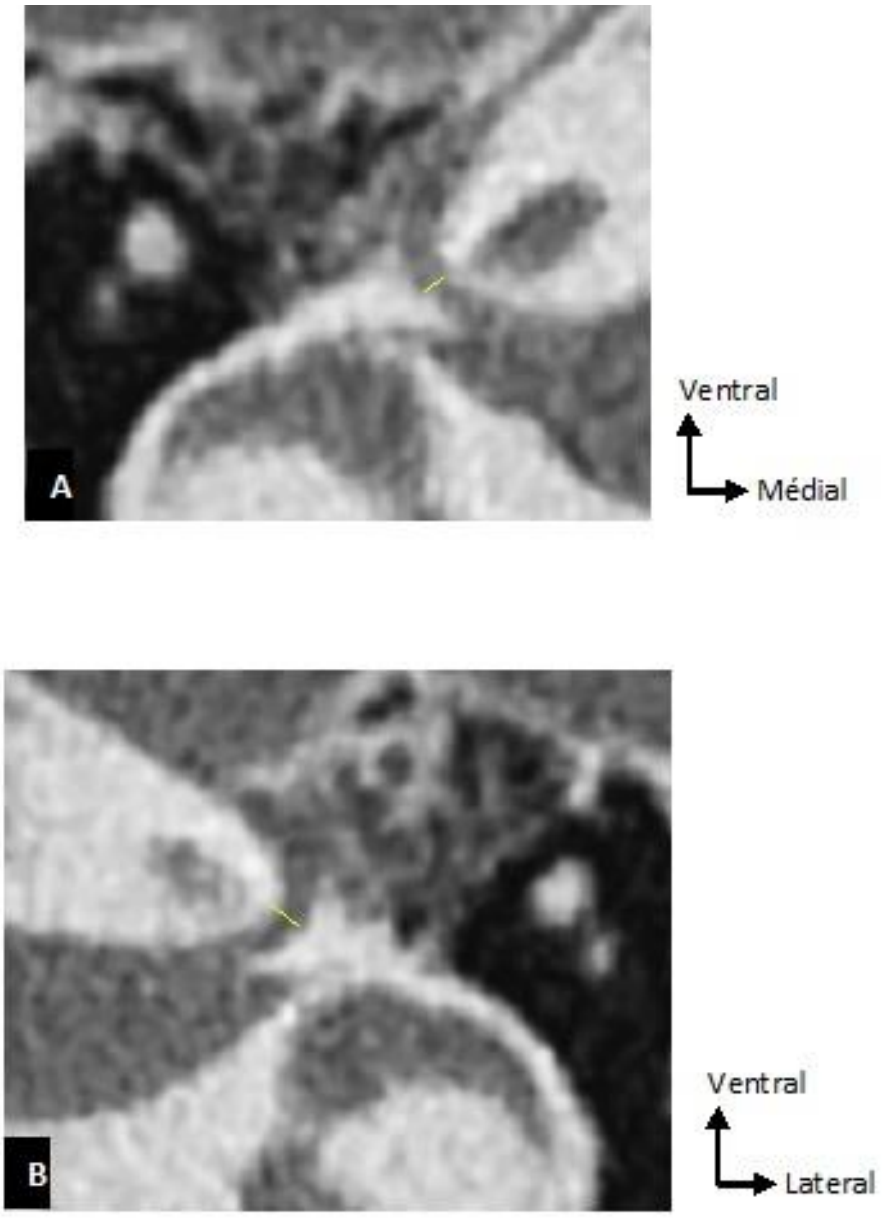

Fig. 4 : Illustration of the measurement of the diameter of the labyrinthine segment of the facial canal on an axial slice of the petrous bone. The measurement is made on a straight line linking the anterior and posterior edges of the facial nerve canal. A. Right petrous bone; B. Left petrous bone.

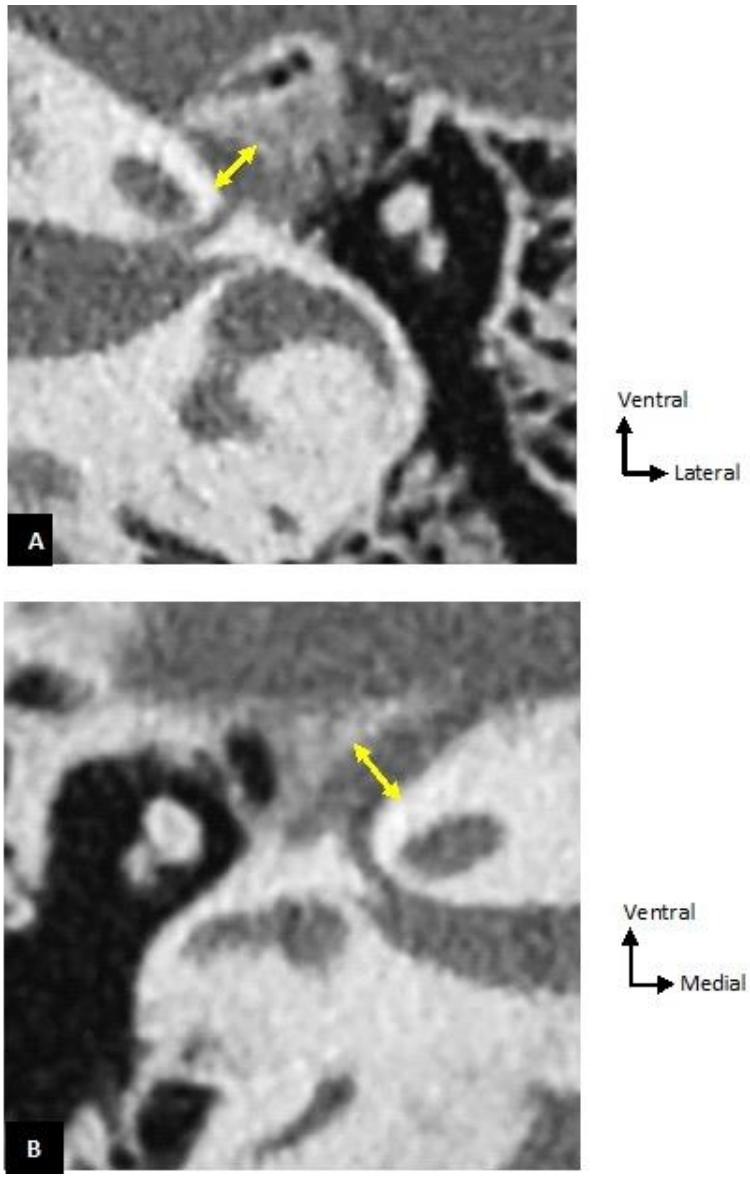

Fig. 5 : Illustration of the measurement of the diameter of the geniculate ganglion fossa on an axial slice of the petrous bone (Yellow arrow). A. Left petrous bone; B. Right petrous bone. The diameter is measured by connecting its medial edge to the lateral one.

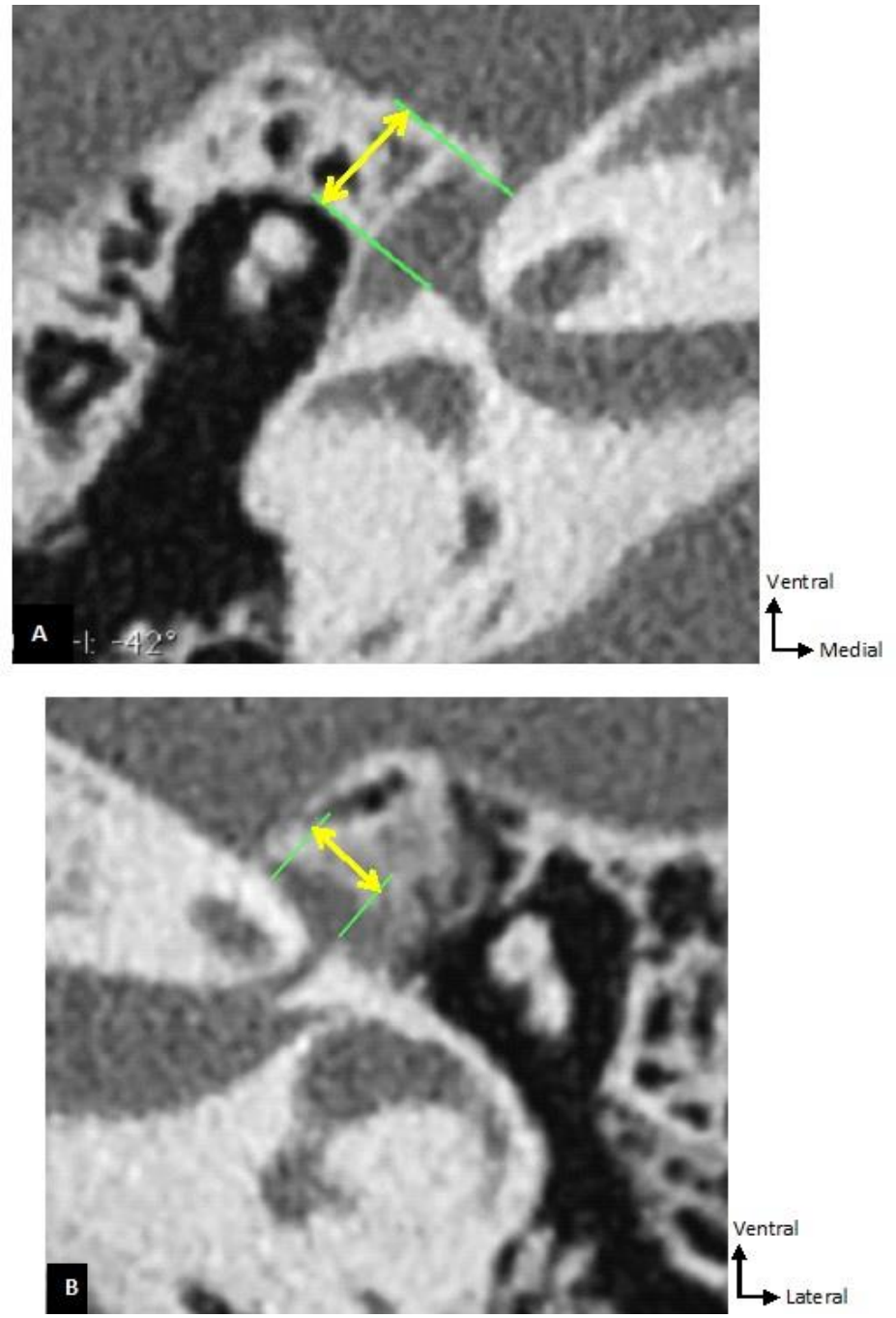

Fig. 6: Illustration of the measurement of the length of the geniculate ganglion fossa on an axial slice of the petrous bone (Yellow arrow). A. Right petrous bone; B. Left petrous bone. The measurement is performed by connecting the anterior end of the fossa (origin of the greater superficial petrosal nerve) to its posterior end (origin of the tympanic segment of the facial nerve canal).

REFERENCES

1. CELIK O, ESKIIZMIR G, PABUSCU Y, ULKUMEN B, TOKER GT. O papel do diâmetro do canal facial na patogenia e grau de paralisia de Bell: estudo por tomografia computadorizada de alta resolução. *Braz J Otorhinolaryngol*. 2017;83(3):261-268. doi:10.1016/j.bjorl.2016.03.016
2. CHEN JY, MAFEE MF. Computed tomography imaging technique and normal computed tomography anatomy of the temporal bone. *Oper Tech Otolaryngol – Head Neck Surg*. 2014;25(1):3-12. doi:10.1016/j.otot.2013.11.002
3. DOBOZI M. Surgical anatomy of the geniculate ganglion. *Acta Otolaryngol*. 1975;80(1-6):116-119. doi:10.3109/00016487509121309
4. ELISABETHINEN K DER. Surgical Radiologic Anatomy multiplanar angulated 2-D-high-resolution CT-reconstruction. Published online 1994:423-427.
5. GUPTA S, MENDS F, HAGIWARA M, FATTERPEKAR G, ROEHM PC. Imaging the Facial Nerve: A Contemporary Review. *Radiol Res Pract*. ;2013:1-14. doi:10.1155/2013/248039
6. HOUSE WF. Surgical Exposure of the Internal Auditory Canal and Its Contents Through the Middle Cranial Fossa. *Laryngoscope*. 1961;71:1363-1385.
7. HOUSE WF, HITSELBERGER W. The middle fossa approach for removal of small acoustic tumors. *Acta Otolaryngol*. 1969;138(3):272-287. doi:10.1080/00016489.2018.1438156
8. HOUSE WF, SHELTON C. Middle Fossa Approach for Acoustic Tumor Removal. *Neurosurg Clin N Am*. 2008;19(2):279-288. doi:10.1016/j.nec.2008.02.009
9. ISAACSON B, VRABEC JT. The radiographic prevalence of geniculate ganglion dehiscence in normal and congenitally thin temporal bones. *Otol Neurotol*. 2007;28(1):107-110. doi:10.1097/01.mao.0000235968.53474.77
10. JÄGER L, REISER M. CT and MR imaging of the normal and pathologic conditions of the facial nerve. *Eur J Radiol*. 2001;40(2):133-146. doi:10.1016/S0720-048X(01)00381-3
11. JIN A, XU P, QU F. Variations in the labyrinthine segment of facial nerve canal revealed by high-resolution computed tomography. *Auris Nasus Larynx*. 2018;45(2):261-264. doi:10.1016/j.anl.2017.05.022
12. LANG J. Cerebellopontine angle, porus and internal acoustic meatus. In: Lang Y, ed. *Clinical Anatomy of the Posterior Cranial Fossa and Its Foramina*. Thieme Medical Publishers; 1991:83-91.
13. MU X, QUAN Y, SHAO J, LI J, WANG H, GONG R. Enlarged Geniculate Ganglion Fossa. CT Sign of Facial Nerve Canal Fracture. *Acad Radiol*. 2012;19(8):971-976. doi:10.1016/j.acra.2012.03.025
14. VALAVANIS A, KUBIK S, OGUZ M. Exploration of the facial nerve canal by high-resolution computed tomography: Anatomy and pathology. *Neuroradiology*. 1983;24(3):139-147. doi:10.1007/BF00347831
15. VEILLON F, RAMOS-TABOADA L, ABU-EID M, CHARPIOT A, RIEHM S. Imaging of the facial nerve. *Eur J Radiol*. 2010;74(2):341-348. doi:10.1016/j.ejrad.2009.08.027
16. VEILLON F, RAMOS L, ABU EID M, ET AL. Imagerie du nerf facial. In: *Imagerie de l'oreille et de l'os Temporal – Tome 4 : Tumeurs, Nerf Facial*. Lavoisier. Médecine Sciences; 2014:989–1041.
17. VEILLON F, TOMASINELLI F, WILLIAM M, SICK H, MOULIN G, MERIOT P. Anatomie normale de l'os temporal. *EMC-Radiologie Imag Médicale Musculo-squelettique-Neurologique-Maxillofaciale*. 1994;7(2).
18. VEILLON F, WILLIAM M, CASSELMANN J, ET AL. Imagerie de l'os temporal normal. In: *EMC-Radiologie et Imagerie Médicale : Musculo-Squelettique-Neurologique-Maxillofaciale*. ; 1994.
19. WADIN K, THOMANDER L, WILBRAND H. The labyrinthine portion of the facial canal in patients with bell's palsy investigated by computed tomography. *Acta radiol*. 1987;28(1):25-30. doi:10.1177/028418518702800105
20. WADIN K, WILBRAND H. A comparative radioanatomic investigation. 1987;28(February 1986):17-23.
21. XIAN-XI GE, SPECTOR GJ. Labyrinthine segment and geniculate ganglion of facial nerve in fetal and adult human temporal bones. *Ann Otol Rhinol Laryngol*. 1981;90(4 II Suppl. 85):1-12. doi:10.1177/00034894810900s401